Low-lying states in the unbound ^{11}N nucleus

E. Casarejos,[1] C. Angulo,[1] P. J. Woods,[2] F. C. Barker,[3] P. Descouvemont,[4] M. Aliotta,[2] T. Davinson,[2] P. Demaret,[1] M. Gaelens,[1,*] P. Leleux,[1] Z. Liu,[2] M. Loiselet,[1] A. S. Murphy,[2] A. Ninane,[1] I. A. Roberts,[2] G. Ryckewaert,[1] J. S. Schweitzer,[5] and F. Vanderbist[1]

[1]*Centre de Recherches du Cyclotron and Institut de Physique Nucléaire, Université Catholique de Louvain, B-1348 Louvain-la-Neuve, Belgium*

[2]*School of Physics and Astronomy, University of Edinburgh, Edinburgh EH9 3JZ, United Kingdom*

[3]*Department of Theoretical Physics, Research School of Physical Sciences and Engineering, Australian National University, Canberra ACT 0200, Australia*

[4]*Physique Nucléaire Théorique et Physique Mathématique CP229, Université Libre de Bruxelles, B-1050 Brussels, Belgium*

[5]*Laboratory for Nuclear Science, University of Connecticut, Storrs, Connecticut 06269-3046, USA*

(Received 1 July 2005; published 31 January 2006)

We have investigated the low-energy states of ^{11}N by the resonant elastic-scattering method in inverse kinematics using a ^{10}C beam and a $(CH_2)_n$ target at the CYCLONE facility at Louvain-la-Neuve. Recoil protons were detected at laboratory angles $\theta_{lab} = 5.2^\circ$–18.3° in a ΔE-E detector system. The absolute ^{10}C+p elastic cross-section data were analyzed in the R-matrix framework. We found ^{11}N to be unbound with respect to proton emission by 1.54 ± 0.02 MeV, with a decay width of 0.83 ± 0.03 MeV. These results are used to calculate the two-proton decay width of the ^{12}O ground state.

DOI: 10.1103/PhysRevC.73.014319 PACS number(s): 21.10.−k, 23.50.+z, 24.30.−v, 27.20.+n

I. INTRODUCTION

The properties of light exotic nuclei are a major source of interest in nuclear physics research [1]. *Ab initio* calculations have now been applied to all nuclei up to mass number $A = 10$ [2] and have revealed important insights such as the need for including three-body interaction terms to reproduce energy level structures. The properties of $A = 11$ nuclei will represent a key challenge for future calculations. Members of the $A = 11$ isobaric chain have already produced startling new insights into nuclear structure. The ^{11}Li nucleus provided the first evidence for the (two-)neutron halo [3,4]. It exhibits a three-body Borromean cluster structure and displays the most diverse range of nuclear decay chains found in nature. Its neighbor ^{11}Be shows the most famous case of nuclear shell inversion (between the $1/2^+$ ground state and $1/2^-$ first excited state), and its ground state has been found to have a one-neutron halo structure. On the proton-rich side ^{11}N, the mirror nucleus of ^{11}Be, is unstable to one-proton decay. Understanding the low-energy resonances of ^{11}N is an important test of nuclear models [5,6]. Furthermore, the energy of the ^{11}N ground state is one of the most important ingredients in predicting the two-proton decay width of the ground state of ^{12}O [7–10].

Much experimental effort has been devoted to elucidating the low-energy resonance structure of ^{11}N [11–16], but there remains considerable disagreement between experimental results and with theoretical predictions [5,6,17–19], particularly with respect to the ground state.

The present paper presents a new, high-precision study of the low-energy resonances of ^{11}N. In Sec. II, the experimental method is described. The data analysis is presented in Sec. III. In Sec. IV, a discussion of the results and a comparison with previous results are presented. Some conclusions are given in Sec. V.

II. EXPERIMENTAL METHOD

We have used the technique of elastic scattering in inverse kinematics [20] to investigate the ^{11}N nucleus. An isobarically pure ^{10}C beam was developed at the CYCLONE radioactive beam facility for the first time, specifically for this experiment. The ^{10}C atoms were produced through the ^{10}B$(p,n)^{10}$C reaction by bombarding a natural boron nitride target with an intense 30 MeV proton beam produced by the CYCLONE30 cyclotron, and these were then ionized to the 2^+ state in an Electron Cyclotron Resonance (ECR) source before being post-accelerated by the CYCLONE110 cyclotron. The ^{10}C beam was stopped 1.5 m downstream from the target in a Faraday cup equipped with a current amplifier suitable to work with low-beam current and with an electron-suppression system. The averaged intensity on target was typically 3×10^4 pps.

We used beams of $E_{lab} = 25.5$ and 32 MeV to bombard a 3 mg/cm^2 polyethylene $(CH_2)_n$ foil. The c.m. energy range covered by the present experiment was $E_{c.m.} = 0.7$–2.8 MeV, with respect to the ^{10}C+p threshold, allowing the study of the $1/2^+$ and $1/2^-$ states in ^{11}N. The target thickness was chosen such that the expected full width of the $1/2^+$ ground state could be encompassed at a single beam energy, while limiting the total energy straggling of the beam in the target. Figure 1 shows a schematic layout of the experimental setup. The recoil protons were detected using a compact disk silicon strip detector based ΔE-E telescope array called CD-PAD which allows for very clean separation between proton, α, and β particles [21]. No signals indicating heavier ions were observed in the ΔE-E telescope. The beam energy was cross-checked with the measured value of the most energetic proton observed. The nominal and measured laboratory energies

*Present address: IBt Int. Brachytherapy, B-7180 Seneffe, Belgium.

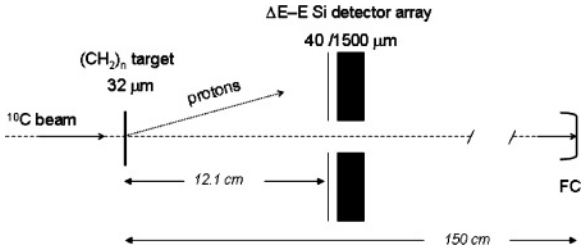

FIG. 1. Schematic layout of the experimental setup. ^{10}C passed through a 32 μm polyethylene target and was stopped in a Faraday cup (FC). Recoil protons were detected on a ΔE-E detector array (see text).

agreed within ±100 keV (better than 0.4%), and the total beam energy spread was less than 100 keV full width at half maximum (FWHM). The CD-PAD array was situated 12.1 cm downstream from the target, covering a laboratory angular range of $\theta_{\rm lab} = 4.6^\circ$–$18.9^\circ$ in 16 strips. The energy calibration of the detector array was performed by means of a three-line α source (^{239}Pu, ^{241}Am, ^{244}Cm) and a precision pulser. The laboratory proton energy resolution was 55 keV for the ΔE detectors and 90 keV for the PAD detectors. The combined energy resolution was $\delta E_e = 105$ keV. Compared with earlier ^{10}C+p studies [12,14], the present improved setup allows better energy and angular resolutions and, because the beam energy is lower and the target thinner, probably a smaller energy straggling. On the other hand, the energy range investigated is smaller here, as we concentrate mainly on the properties of the $1/2^+$ ^{11}N ground state.

Two important effects have to be taken into account in the data analysis. First, the opening angle of the detector strips introduces an uncertainty in the proton energy given by $\delta E_\theta = 2E_p \tan\theta_{\rm lab}\Delta\theta_{\rm lab}$ [22]. Typical values range between 20 and 160 keV (for the proton energies and angles covered). The second effect is the straggling of the beam particles and of the recoil protons in the target. The most important straggling effect is that of the beam in the target, which produces an additional uncertainty in the laboratory energies of the recoil protons, typically of less than 6%. The total energy broadening is obtained by adding quadratically all contributions, and it is one of the inputs in the theoretical analysis of the cross section (Sec. III).

Figure 2 shows a raw ΔE-E spectrum obtained at the beam energy of 25.5 MeV (spectra for 32 MeV are similar). Recoil protons from the ^{10}C+p elastic scattering are clearly separated from α particles resulting from reactions of ^{10}C with the C content in the target. This spectrum shows that the use of polyethylene targets is perfectly suitable for this kind of experiment provided the appropriate detector system is used. A detailed simulation of the proton spectra was performed including the energy loss [23] and the energy straggling of the ^{10}C beam and the protons in the target. The pulse height defect effect due to the different energy deposition in the detector by protons with respect to α particles (below 1%) [24] as well as the beam energy spread were also included.

From the recoil proton spectra, we obtained absolute differential cross sections for 10 effective laboratory angles (recoil spectra of the 12 innermost strips were added two

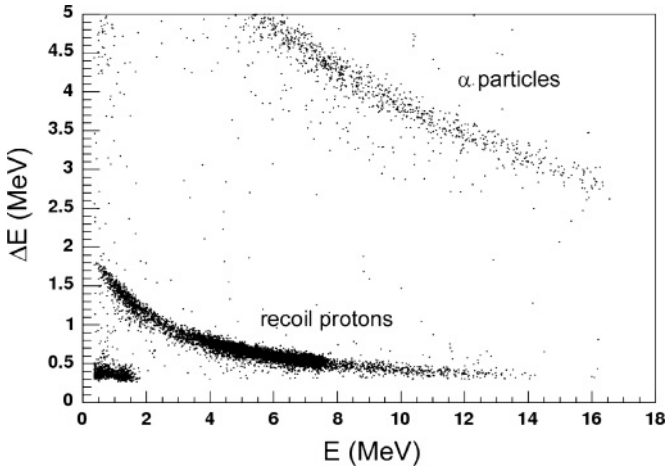

FIG. 2. Example of ΔE vs E spectrum obtained for a 25.5 MeV ^{10}C beam. The spectrum is obtained by adding the signals from adjacent strips in the angular range of $\theta_{\rm lab} = 6.7^\circ$–$12.6^\circ$. Signals with $\Delta E < 0.5$ MeV are β particles from the ^{10}C decay.

by two) in the range $\theta_{\rm lab} = 5.2^\circ$–$18.3^\circ$ and for c.m. energies $E_{\rm c.m.} = 0.7$–2.75 MeV by correcting the number of counts for the solid angle of the detectors (±5%), the H content in the target (±10%), and the total number of incident beam particles (±15%). This last quantity is the most critical one to obtain an absolute normalization. We used the Rutherford elastic scattering of the ^{10}C beam in a Au target to calibrate the current amplifier at the Faraday cup. Charge-state distribution was calculated based on the method described in Ref. [25]. This technique has been successfully used in several experiments (see, for example, Ref. [26]). Figure 3 shows the cross section as a function of the c.m. energy for three typical angles $\theta_{\rm c.m.} = 143.5^\circ$, 158.5°, and 169.7° [27].

III. DATA ANALYSIS

A. Resonance parameters

We used the R-matrix model [28] in the one-channel, one-level approximation to fit the differential cross sections in the 143.5°–169.7° c.m. angular range and 0.7–2.75 MeV c.m. energy range ($N = 398$ data points). In the R-matrix framework, the nuclear phase shift is defined by

$$\delta^\ell = \delta^\ell_{\rm HS} + \delta^\ell_R, \tag{1}$$

where $\delta^\ell_{\rm HS}$ is the hard-sphere phase shift and δ^ℓ_R is the resonant phase shift given by

$$\delta^\ell_R = \arctan\frac{P_\ell R^\ell}{1 - S_\ell R^\ell}, \tag{2}$$

where P_ℓ and S_ℓ are the penetration and shift factors, respectively (we have assumed the boundary condition $B_\ell = 0$). The R-matrix R^ℓ defined in the one-level approximation is given by

$$R^\ell = \frac{\gamma^2_\ell}{E_\ell - E}, \tag{3}$$

with γ_ℓ and E_ℓ the formal reduced width amplitude and the energy of the R-matrix pole, respectively.

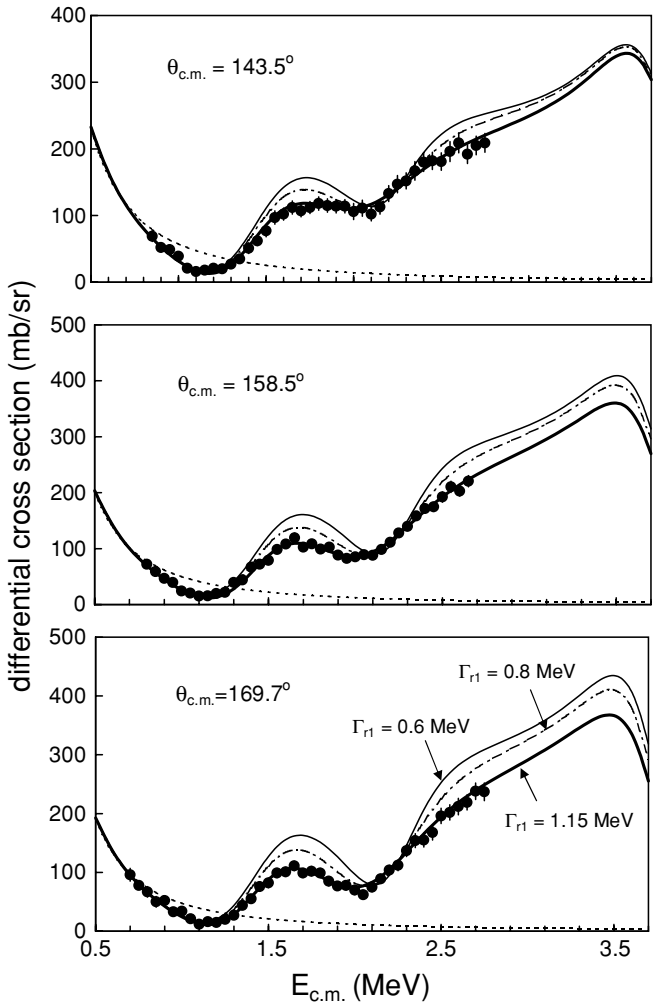

FIG. 3. Elastic cross section vs c.m. energy for the system $^{10}C+p$ for three typical c.m. angles. Error bars are statistical only. Thick solid curves are the best simultaneous R-matrix fits to data at all angles of Table I ($a = 6.25$ fm, $\chi^2 = 231$, $\xi = 1.0$, $N = 398$). Thin solid (dotted-dashed) curves are R-matrix calculations with $\Gamma_{r1} = 0.6$ MeV (0.8 MeV), and with the other parameters fixed at their values of the best fit in Table I. The dotted curves are the Rutherford cross sections.

The observed resonant width, which should be compared with the experimental width, is given by

$$\Gamma_{r\ell} = \frac{\Gamma_\ell}{1 + \gamma_\ell^2 (dS_\ell/dE)_{E_{r\ell}}}, \tag{4}$$

where $E_{r\ell}$ is the resonance energy defined as the energy at which δ_R^ℓ passes through $\pi/2$, and Γ_ℓ is the formal width of the R-matrix pole defined by

$$\Gamma_\ell = 2\gamma_\ell^2 P_\ell(E_{r\ell}). \tag{5}$$

For broad resonances, as expected in ^{11}N, the peak energy E_m and the peak width Γ_m are also used to characterize the states differently from the resonant energy $E_{r\ell}$ and resonant width $\Gamma_{r\ell}$. The peak energy is the energy where the density-of-states function ρ reaches the maximum, with $\rho = \sin^2\delta_R^\ell / P_\ell$ [29]; the peak width is defined as the FWHM of the peak.

Here, ℓ values up to $\ell_{\max} = 3$ have been included. We have included resonance contributions for partial waves ℓ, $J = 0, 1/2; 1, 1/2; 2, 5/2$ and used hard-sphere phase shifts for other ℓJ values (see Ref. [30] for more details). The fitted parameters are the pole parameters E_ℓ, Γ_ℓ ("calculated" parameters) converted to the resonance energies $E_{r\ell}$, and proton widths $\Gamma_{r\ell}$ ("observed" parameters) of the ^{11}N states [31,32]. In order to account for the experimental energy spread described above, we convoluted the calculations at each angle with a Gaussian energy distribution, with a FWHM set equal to the total experimental energy broadening at that angle (c.m. values ranging from 120 to 160 keV). For resonances with large widths, the resulting parameters depend slightly on these values; only the χ^2 values depend.

The fits are performed with different values of the R-matrix channel radius $a = 5.5$–7.0 fm. Because the data do not extend to the energy of the $5/2^+$ state, we fixed its resonance energy and width at 3.70 ± 0.05 and 0.55 ± 0.05 MeV, respectively. These are the weighted averaged values of Table IV in Ref. [14] and Table II in Ref. [16]. The remaining free parameters are the resonance energies and decay widths of the $1/2^+$ and $1/2^-$ states (E_{r0}, Γ_{r0}, E_{r1}, Γ_{r1}). The influence of the absolute normalization, the choice of the channel radius a, the uncertainties of the $5/2^+$ state parameters, and the uncertainty associated with the experimental energy spread were carefully studied by performing R-matrix fits for different initial conditions. For each fit, the uncertainties in the fitted parameters are calculated from the R-matrix fits that have $\chi^2 = \chi^2_{\min} + 1$. Table I shows the fits for different values of the channel radius a. Similar results are obtained when the normalization, the parameters of the $5/2^+$ state, and the energy spread are varied. We have found that all parameters depend only slightly on these conditions, with the exception of Γ_{r1}. Figure 4 shows the variation of χ^2 with a normalization factor $\xi = 1.0$ and of ξ (for the best χ^2 values) as a function of a. From the overall study of the effect of the different uncertainties (absolute normalization, value of the channel radius, parameters of the $5/2^+$ state, and experimental energy resolution), we recommend the following values for the parameters of the $1/2^+$ and the

TABLE I. Resonance energies and observed widths from the R-matrix best fits of the $^{10}C+p$ data ($N = 398$ data points), for various values of channel radius a and for fixed values of the resonance energy $E_{r2} = 3.7$ MeV and the observed width $\Gamma_{r2} = 0.55$ MeV of level 3 ($5/2^+$). Level 1 is $1/2^+$, level 2 is $1/2^-$. For each value of a, the uncertainties are calculated from the R-matrix fits that have $\chi^2 = \chi^2_{\min} + 1$.

a (fm)	E_{r0} (MeV)	Γ_{r0} (MeV)	E_{r1} (MeV)	Γ_{r1} (MeV)	$\chi^2_{\min}$
5.5	1.560 ± 0.002	0.831 ± 0.007	2.220 ± 0.004	0.83 ± 0.02	430
5.75	1.552 ± 0.002	0.828 ± 0.006	2.236 ± 0.004	0.93 ± 0.02	322
6.0	1.546 ± 0.002	0.827 ± 0.007	2.255 ± 0.003	1.05 ± 0.02	251
6.25	1.540 ± 0.002	0.827 ± 0.006	2.277 ± 0.003	1.18 ± 0.02	231
6.5	1.535 ± 0.002	0.828 ± 0.007	2.301 ± 0.004	1.32 ± 0.02	287
6.75	1.530 ± 0.002	0.830 ± 0.007	2.329 ± 0.004	1.49 ± 0.02	430
7.0	1.528 ± 0.002	0.840 ± 0.007	2.366 ± 0.004	1.67 ± 0.02	685

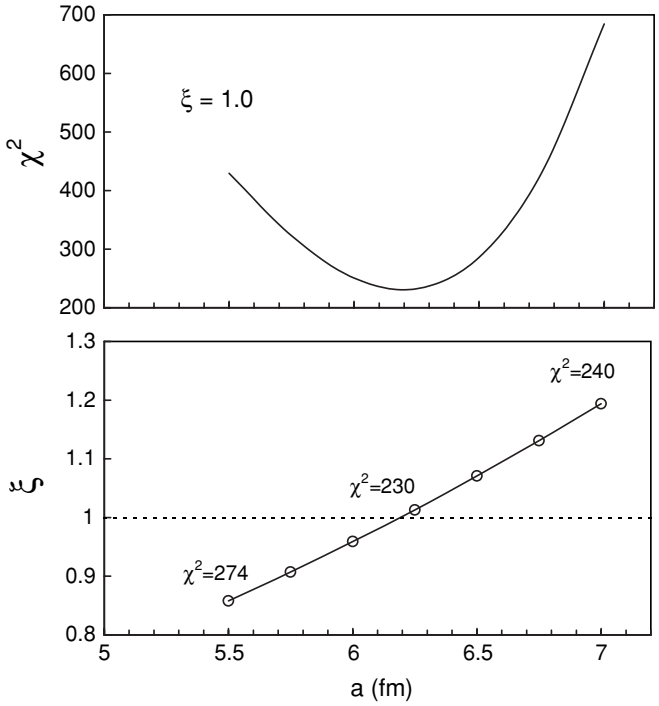

FIG. 4. Variation of χ^2 and the normalization factor ξ with respect to the channel radius a (factor ξ multiplies the experimental cross section).

$1/2^-$ states: $E_{r0} = 1.54(2)$, $\Gamma_{r0} = 0.83(3)$, $E_{r1} = 2.27(5)$, and $\Gamma_{r1} = 1.15(25)$ MeV.

The best fit of Table I ($a = 6.25$ fm, $\chi^2 = 231$) is shown as thick solid curves in Fig. 3. To prove the sensitivity of the fits, we performed R-matrix calculations (no fits) with a, E_{r0}, Γ_{r0}, and E_{r1} fixed at their values of the best fit of Table I, but using different values for Γ_{r1}. These calculations are shown in Fig. 3 for $\Gamma_{r1} = 0.6$ and for $\Gamma_{r1} = 0.8$ MeV. These curves are in clear disagreement with the data. Similar results are obtained by varying E_{r0}, Γ_{r0}, or E_{r1}.

As an illustration, Table II gives a comparison of the experimental parameters, the formal parameters, and the peak parameters of the $\ell = 0$, 1 low-energy levels of ^{11}N for typical values of the channel radius a.

B. Spectroscopic factors

In order to obtain values of the spectroscopic factors $\mathcal{S}_\ell$, we used [33,34]

$$\Gamma_\ell = \mathcal{S}_\ell \Gamma_{\mathrm{sp},\ell}, \tag{6}$$

TABLE III. Spectroscopic factors of the $1/2^+$ and $1/2^-$ states in ^{11}N (a is in fm, γ_i^2 in MeV).

a	γ_0^2	$\mathcal{S}_0$	γ_1^2	$\mathcal{S}_1$
5.75	0.572	0.46	0.681	1.00
6.25	0.497	0.50	0.704	1.25
6.75	0.440	0.55	0.738	1.52

where the single-particle width $\Gamma_{\mathrm{sp},\ell}$ is given as a function of the single-particle dimensionless reduced width $\theta^2_{\mathrm{sp},\ell}$ and the penetration factor by

$$\Gamma_{\mathrm{sp},\ell} = 2\gamma^2_{\mathrm{sp},\ell} P_\ell(E_{r\ell}), \quad \gamma^2_{\mathrm{sp},\ell} = \frac{\hbar^2}{\mu a^2}\theta^2_{\mathrm{sp},\ell}, \tag{7}$$

with

$$\theta^2_{\mathrm{sp},\ell} = \frac{a}{2}\frac{u_\ell^2(a)}{\int_0^a u_\ell^2(r)dr}. \tag{8}$$

We calculate the radial wave function $u_\ell(r)$ for a Woods-Saxon potential with conventional parameters [6] ($R_0 = 2.693$ fm, diffuseness $= 0.65$ fm); we found $V_0(1/2^+) = -56.2$ MeV, $V_0(1/2^-) = -30.8$ MeV for $a = 6.25$ fm. Values of $\mathcal{S}_\ell$ are given in Table III for typical values of a. The values of $\mathcal{S}_0$ are about 0.5, to be compared with the shell-model values of 0.76 [6], 0.82 [35], and 0.74 [36] and the experimental values for the ^{11}Be analog level of 0.73 ± 0.06 [37], 0.77 [38], and 0.66–0.79 [39]. Recent theoretical analyses have, however, reported $\mathcal{S}_0$ values of 0.36–0.44 [40] and 0.19 ± 0.02 [41]. The values of $\mathcal{S}_1 \simeq 1.3$ are larger than the shell-model values of 0.60 [42], 0.66 [43], and 0.76 [6], and experimental values for the ^{11}Be analog level of 0.63 ± 0.15 [37], 0.96 [38], and 0.72 ± 0.04 [44]. Notice that, by definition, the rigorous limit on $\mathcal{S}$ is not 1.0 (see, for example, [45]). For the broad $1/2^-$ state, $\mathcal{S}_1$ strongly depends on the channel radius. The definition of the spectroscopic factor for broad resonances is qualitative only, as the wave functions are not square-integrable. Accordingly, the $\mathcal{S}_1$ values should be considered as indicative only.

IV. DISCUSSION

A. Comparison with previous results on low-lying resonances in ^{11}N

For more than 30 years, there has been considerable experimental and theoretical effort to study the low-energy states of ^{11}N. In the pioneering work of Benenson *et al.* [11], a light-ion multinucleon transfer reaction was used; a resonance found at 2.24 MeV was interpreted as the analog of the

TABLE II. Experimental resonance parameters (E_{ri}, Γ_{ri}), formal parameters (E_i, Γ_i), and peak parameters (E_{mi}, Γ_{mi}) of the $1/2^+$ ($\ell = 0$) and $1/2^-$ ($\ell = 1$) states in ^{11}N for different values of the channel radius a (in fm). All energies are in MeV.

a	E_{r0}	Γ_{r0}	E_0	Γ_0	E_{m0}	Γ_{m0}	E_{r1}	Γ_{r1}	E_1	Γ_1	E_{m1}	Γ_{m1}
5.75	1.552	0.828	1.380	0.929	1.489	0.761	2.236	0.933	1.844	0.967	2.171	0.869
6.25	1.540	0.827	1.397	0.914	1.478	0.765	2.277	1.180	1.917	1.228	2.184	1.081
6.75	1.530	0.830	1.410	0.906	1.469	0.770	2.329	1.489	1.995	1.551	2.198	1.329

$1/2^-$ first excited state of ^{11}Be. Axelsson *et al*. [12] reported evidence for the ground and first two excited states of ^{11}N in experiments performed at Grand Accelerateur National d'lons Lourds (GANIL) using a ^{10}C beam produced by heavy-ion fragmentation to bombard an extended methane gas target. Later, the Axelsson *et al*. data were reanalyzed, along with similar data from Michigan State University (MSU), and significantly revised values were published by Markenroth *et al*. [14]. In particular, the ground state was reported at a resonance energy of 1.27 MeV with a decay width of 1.44 MeV. Lépine-Szily *et al*. used the transfer reaction ^{12}C(^{14}N,^{15}C)^{11}N at GANIL [13] and observed the first excited state at 2.18 MeV with a width of 0.44 MeV; no evidence of the ground state was observed. Heavy-ion transfer-reaction studies performed in the Spectromètre à Perte d'Energie du Ganil (SPEG) spectrometer at GANIL by Oliveira *et al*. [15] reported a $1/2^+$ ground state with an energy of 1.63 MeV and a width of 0.4 MeV, in marked disagreement with Ref. [14]. Furthermore, while reasonable agreement was obtained for the energy of the $1/2^-$ first excited state, there was considerable disagreement in its decay widths, 0.84 [14] and 0.25 MeV [15]. In the SPEG experiment, an additional state was reported at an energy of 3.06 MeV that was not observed in Ref. [14], although both experiments reported the observation of the predicted $5/2^+$ second excited state around 3.7 MeV (width ∼0.5 MeV). Finally, Guimarães *et al*. investigated the transfer reaction ^{14}N(^{3}He,^{6}He)^{11}N at RIKEN [16]. The reported ^{11}N ground state energy was 1.31 MeV, in fair agreement with the work of [14], but the decay width of 0.24 MeV was the smallest value ever reported and in strong disagreement with several theoretical predictions [5,6,17–19] (see Table IV). Notice also that the definitions of "energy" and "width" may not be the same in all the prescriptions used to analyze the experimental results [6]. For example, the values reported by [6,12,14,16,18] are more likely peak energies and widths rather than resonance energies and widths. Table IV shows a summary of experimental and theoretical values, including the present work, for the low-lying $1/2^+$ and $1/2^-$ resonances in ^{11}N. As stated above, uncertainties over previous definitions of measured quantities make direct comparisons difficult. However, we can note that the present precise value for the width of the ground state disagrees significantly with all previous results, while the resonance energy appears consistent with that obtained by Oliveira *et al*. [15]. For the $1/2^-$ state a more consistent picture emerges for the resonance energies, with the present value being the most precise of the ^{10}C+p results. The width obtained here is significantly higher than other values and appears to be consistent only with the value reported by Markenroth *et al*. [14], both with comparable uncertainties.

The differences between theoretical calculations are even larger than the differences between experiments because of the very specific nature of ^{11}Be and ^{11}N, where the parity inversion is difficult to reproduce, as in Ref. [17]. Moreover, for broad resonances as in ^{11}N, the definitions of energy and width may depend on the model. For example, Markenroth *et al*. [14] used the potential model for three levels plus a background term to analyze their ^{10}C+p data and different definitions for the energy and width of an unbound level. The present results are deduced from R-matrix fits, which should make a comparison with further models easier.

B. Width of the ^{12}O ground state

The contribution to the width of ^{12}O(g.s.) due to sequential decay through the $1/2^+$ ^{11}N(g.s.) may be calculated as in Ref. [8]. It depends on the value of E_{r0} for ^{11}N and on the reduced width γ_0^2 for $^{12}\mathrm{O(g.s.)} \rightarrow {}^{11}\mathrm{N(g.s.)} + p$. For the conventional values of the channel radii $a_1 = 4.68$, $a_2 = 4.57$ fm [8] and for our recommended value $E_{r0} = 1.54$ MeV, this contribution is proportional to γ_0^2, as in Fig. 1 of Ref. [8], reaching a value of 27 keV for γ_0^2 equal to the Wigner limit of 3.11 MeV (for $a_2 = 6.25$ fm, the upper limit on the contribution is 32 keV).

The present upper limit for the sequential two-proton decay width through the ground state of ^{11}N is inconsistent with the experimental results for the two-proton decay of

TABLE IV. Energies and widths (in MeV) of the $1/2^+$ and $1/2^-$ states in ^{11}N from this work (Table I) and compared to previous results (values of Ref. [12] are superseded by Ref. [14], values of Refs. [6,14,16,18] are peak parameters).

	Experimental results									
	This work		Lépine-Szily [13]		Markenroth [14]		Oliveira [15]		Guimarães [16]	
J^π	E_r	Γ_r	E_r	Γ_r	E_m	Γ_m	E_r	Γ_r	E_m	Γ_m
$\frac{1}{2}^+$	1.54(2)	0.83(3)	–	–	$1.27^{0.18}_{0.05}$	1.44(20)	1.63(5)	0.4(1)	1.31(5)	0.24(24)
$\frac{1}{2}^-$	2.27(5)	1.15(25)	2.18(5)	0.44(8)	2.01(15)	0.84(20)	2.16(5)	0.25(8)	2.31(2)	0.73(6)

	Theoretical results							
	Fortune [5]		Barker [6]		Descouvemont [17]		Grévy [18]	
J^π	E_r[a]	Γ_r[a]	E_m	Γ_m	E_r	Γ_r	E_m	Γ_m
$\frac{1}{2}^+$	1.60	1.58	1.4	1.01	1.1	0.9	1.2	1.1
$\frac{1}{2}^-$	2.48	0.91	2.21	0.74	1.6	0.3	2.1	1

[a]If parameters in Table III of Ref. [5] are equivalent to E_r, Γ_r as defined here.

the ground state of ^{12}O [7,8], which report a width of 578(205) keV with an upper limit of 7% for ^{2}He emission. Barker has already suggested that in fact the ^{12}O experimental width may statistically be consistent with the experimental resolution of the ^{12}O setup [7,8]. Our latest results would lend further support to this possibility and point to the need for a new higher-resolution experimental study of the two-proton decay of ^{12}O to resolve this important issue.

V. CONCLUSIONS

A new ^{10}C beam has been developed at the CYCLONE radioactive beam facility at Louvain-la-Neuve. The method of scattering of protons in inverse kinematics has been used to identify low-lying resonances in the proton unbound nucleus ^{11}N. A detailed *R*-matrix analysis has yielded precise values for the resonance parameters. The value of the resonance energy for the ground state of ^{11}N has been used to obtain an upper limit of the two-proton decay width for ^{12}O. The result supports the present inconsistency between the current experimental two-proton decay width for ^{12}O and a predominant sequential decay through the ground state of ^{11}N.

ACKNOWLEDGMENTS

We are grateful to the CRC staff for the production of the ^{10}C beam and the technical support during the experiment. We thank B. Jonson for useful discussions. This work has been supported by the Belgian program P5/07 on inter-university attraction poles of the Belgian-State Federal Services for Scientific, Technical and Cultural Affairs and the UK Engineering & Physical Science Research Council (EPSRC). M.G., P.D., and P.L. acknowledge the support of the National Fund for Scientific Research (FNRS), Belgium.

[1] B. Jonson, Phys. Rep. **389**, 1 (2004).
[2] S. C. Pieper, K. Varga, and R. B. Wiringa, Phys. Rev. C **66**, 044310 (2002).
[3] I. Tanihata, H. Hamagaki, O. Hashimoto, Y. Shida, N. Yoshikawa, K. Sugimoto, O. Yamakawa, T. Kobayashi, and N. Takahashi, Phys. Rev. Lett. **55**, 2676 (1985).
[4] P. G. Hansen, A. S. Jensen, and B. Jonson, Annu. Rev. Nucl. Part. Sci. **45**, 591 (1995).
[5] H. T. Fortune, D. Koltenuk, and C. K. Lau, Phys. Rev. C **51**, 3023 (1995).
[6] F. C. Barker, Phys. Rev. C **53**, 1449 (1996).
[7] R. A. Kryger *et al.*, Phys. Rev. Lett. **74**, 860 (1995).
[8] F. C. Barker, Phys. Rev. C **59**, 535 (1999).
[9] R. Sherr and H. T. Fortune, Phys. Rev. C **60**, 064323 (1999).
[10] F. C. Barker, Phys. Rev. C **63**, 047303 (2001).
[11] W. Benenson *et al.*, Phys. Rev. C **9**, 2130 (1974).
[12] L. Axelsson *et al.*, Phys. Rev. C **54**, R1511 (1996).
[13] A. Lépine-Szily *et al.*, Phys. Rev. Lett. **80**, 1601 (1998).
[14] K. Markenroth *et al.*, Phys. Rev. C **62**, 034308 (2000).
[15] J. M. Oliveira *et al.*, Phys. Rev. Lett. **84**, 4056 (2000).
[16] V. Guimarães *et al.*, Phys. Rev. C **67**, 064601 (2003).
[17] P. Descouvemont, Nucl. Phys. **A615**, 261 (1997).
[18] S. Grévy, O. Sorlin, and N. Vinh Mau, Phys. Rev. C **56**, 2885 (1997).
[19] R. Sherr and H. T. Fortune, Phys. Rev. C **64**, 064307 (2001).
[20] C. Angulo, Nucl. Phys. **A746**, 222c (2004).
[21] A. N. Ostrowski *et al.*, Nucl. Instrum. Methods A **480**, 448 (2002).
[22] R. Coszach *et al.*, Phys. Lett. **B353**, 184 (1995).
[23] J. F. Ziegler and J. P. Biersack, SRIM 2000 program, version 39, 1998, IBM Co, 1999.
[24] W. N. Lennard *et al.*, Nucl. Instrum. Methods A **248**, 454 (1886).
[25] T. K. Chaki and D. Elmore, Semi-empirical formulas and tables for charge state distributions in gas and solid strippers, Nuclear Structure Research Laboratory Report 24, University of Rochester (1980).
[26] R. Raabe *et al.*, Nature (London) **431**, 823 (2004).
[27] Data for all measured angles are available upon request.
[28] A. M. Lane and R. G. Thomas, Rev. Mod. Phys. **30**, 257 (1958).
[29] F. C. Barker, Aust. J. Phys. **40**, 307 (1987).
[30] C. Angulo *et al.*, Nucl. Phys. **A716**, 211 (2003).
[31] C. Angulo and P. Descouvemont, Phys. Rev. C **61**, 064611 (2000).
[32] C. R. Brune, Phys. Rev. C **66**, 044611 (2002).
[33] A. M. Lane, Rev. Mod. Phys. **32**, 519 (1960).
[34] M. H. MacFarlane and J. B. French, Rev. Mod. Phys. **32**, 567 (1960).
[35] W. D. Teeters and D. Kurath, Nucl. Phys. **A275**, 61 (1977).
[36] T. Aumann *et al.*, Phys. Rev. Lett. **84**, 35 (2000).
[37] D. L. Auton, Nucl. Phys. **A157**, 305 (1970).
[38] B. Zwieglinski *et al.*, Nucl. Phys. **A315**, 124 (1979).
[39] S. Fortier *et al.*, Phys. Lett. **B461**, 22 (1999).
[40] N. K. Timofeyuk and R. C. Johnson, Phys. Rev. C **59**, 1545 (1999).
[41] R. C. Johnson *et al.*, in *Experimental Nuclear Physics in Europe*, edited by Berta Rubio, Manuel Lozano, and William Gelletly, AIP Conf. Proc. No. 495 (AIP, Melville, NY, 1999), p. 297.
[42] S. Cohen and D. Kurath, Nucl. Phys. **A101**, 1 (1967).
[43] P. D. Hauge and S. Maripuu, Phys. Rev. C **8**, 1609 (1973).
[44] N. Fukuda *et al.*, Phys. Rev. C **70**, 054606 (2004).
[45] A. M. Mukhamedzhanov, C. A. Gagliardi, and R. E. Tribble, Phys. Rev. C **63**, 024612 (2001).